Analytical Methods

PAPER

View Article Online
View Journal | View Issue

Cite this: *Anal. Methods*, 2018, **10**, 5313

Sensitive detection of bisphenol A in drinking water and river water using an upconversion nanoparticles-based fluorescence immunoassay in combination with magnetic separation†

Wei Sheng, *[a] Wenxia Duan,[a] Yingjie Shi,[a] Qing Chang,[a] Yan Zhang,[a] Yang Lu[a] and Shuo Wang*[ab]

We have proposed a sensitive fluorescence immunoassay for detecting bisphenol A (BPA) in barreled drinking water, bottled mineral water, and river water using the anti-BPA antibody conjugated carboxyl-functionalized $NaYF_4$:Yb/Tm upconversion nanoparticles (UCNPs) (emission maximum at 454 nm with excitation at 980 nm) as the signal probe and the coating antigen conjugated carboxyl-functionalized magnetic polystyrene microspheres (MPMs) as the capture probe. The proposed assay has a linear detection range of 0.1 to 500 μg L^{-1} (R^2 = 0.9954). The water samples without any pretreatment can be directly analyzed. The limit of detection (LOD) of BPA in the water samples is 0.02 μg L^{-1}. The recoveries of BPA from spiked water samples for the proposed assay range from 85.35% to 108.35%. Low concentrations of BPA have been detected in the real barreled drinking water and river water samples, and the results are validated by high-performance liquid chromatography (HPLC) to be reliable, reflecting the good practicability of the proposed assay. The proposed fluorescence immunoassay can serve as a useful detection approach for the simple, rapid, sensitive, and accurate determination of BPA in drinking and environmental water.

Received 3rd June 2018
Accepted 17th October 2018

DOI: 10.1039/c8ay01260a

rsc.li/methods

1. Introduction

Bisphenol A (BPA) is an important monomer component in producing epoxy resins, polycarbonate plastics, and flame retardants.[1,2] However, BPA is a recognized endocrine disruptor.[3,4] It can enter organisms *via* the food chain, thus interacting with estrogen receptors to affect the physiological functions of organisms.[5] The discharge of the wastewater containing BPA into the environment and the release and transfer of BPA from packing materials to drinking water or food can cause BPA contamination.[6] Therefore, it is necessary to develop a useful detection approach for monitoring BPA in consideration of its potential hazard to human health and the ecological environment.

A variety of methods have been established for detecting BPA, including high-performance liquid chromatography[7] coupled with mass spectrometry,[8] gas chromatography–mass spectrometry,[9] surface-enhanced Raman spectroscopy,[10] capillary electrophoresis,[11] and electrochemical sensing.[12] Compared with these analytical methods, the immunoassay has some advantages, mainly containing high sensitivity and selectivity for target recognition, short detection time, fast signal output, and good anti-interference ability for the matrix. Their main methods are the enzyme-linked immunosorbent assay (ELISA),[13,14] immunochromatographic assay,[15,16] electrochemical immunosensing,[17] surface plasmon resonance biosensing,[18] surface-enhanced Raman spectroscopy (SERS) based immunoassay,[19] chemiluminescence immunoassay[20] and fluorescence immunoassay,[21–24] which have been successfully used for detecting BPA in water and food samples.

The immunoassay based on fluorescence nanomaterials has attracted great attention with researchers. Conventional down-conversion fluorescence materials, such as organic dyes[25] and quantum dots,[24] are commonly used in biological analysis and other diverse applications based on their unique optical properties. However, they also have several minor defects. The luminescence process is a conversion of high-frequency excitation light to low-frequency emission light, which means that it radiates less energy than it absorbs. The use of higher-energy light may cause significant disadvantages including low light penetration depth, potential light damage to living tissue,[26] and

[a]*State Key Laboratory of Food Nutrition and Safety, Key Laboratory of Food Nutrition and Safety, Ministry of Education of China, College of Food Engineering and Biotechnology, Tianjin University of Science and Technology, Tianjin 300457, China. E-mail: shengweijunchen@163.com; s.wang@tust.edu.cn; Fax: +86 22 6091 2489; Tel: +86 22 6091 2483*

[b]*Beijing Advanced Innovation Center for Food Nutrition and Human Health, Beijing Technology & Business University (BTBU), Beijing 100048, China*

† Electronic supplementary information (ESI) available. See DOI: 10.1039/c8ay01260a

unstable optical and chemical features.[27] To solve these problems, upconversion nanoparticles (UCNPs) adulterating lanthanide have been applied as a biological luminescent label. The upconversion nanomaterial has successfully attracted attention due to its superior optical performances compared to the abovementioned downconversion material, such as large anti-Stokes shift, high resistance to photobleaching, strong light penetration of biological tissue, very good biocompatibility and excellent chemical stability, and low toxicity.[28–30] A few studies applying UCNPs as fluorescence labels for detecting bacteria, mycotoxins, protein, and antibiotics have been reported recently.[29–32] In our study, we have proposed a sensitive fluorescence immunoassay for detecting BPA in drinking and river water using UCNPs as fluorescence labels to prepare the signal probe and the magnetic polystyrene microspheres (MPMs) as separation component to prepare the capture probe.

2. Materials and methods

2.1. Chemicals and materials

Bisphenol A (BPA), 4,4-bis(4-hydroxyphenyl)valeric acid (BHPVA) (the structures of BPA and BHPVA are shown in ESI Fig. S1†), $C_6H_9O_6Yb\cdot 4H_2O$, $C_6H_9Tm\cdot 4H_2O$, $Y(OOCCH_3)_3\cdot 4H_2O$, polyacrylic acid (PAA), diethylene glycol (DEG), bovine serum albumin (BSA), ovalbumin (OVA), 1-ethyl-3-[3-(dimethylamino) propyl]carbodiimide (EDC), *N*-hydroxysuccinimide (NHS), and dimethyl sulfoxide (DMSO) were purchased from Sigma-Aldrich Co. Ltd. (St. Louis, MO, USA). Sodium hydroxide, ammonium fluoride, 1-octadecene (ODE, 90%), and oleic acid (OA, 90%) were purchased from Sinopharm Chemical Reagent Co. Ltd. (Tianjin, China). The anti-BPA polyclonal antibody using BHPVA-keyhole limpet hemocyanin conjugate as an immunogen was produced in our laboratory. The BCA protein quantification kit was purchased from Solarbio Science and Technology Co., Ltd. (Beijing, China). The carboxyl-functional magnetic polystyrene microspheres (MPMs) were obtained from Jiayuan Quantum Dots Co., Ltd. (Wuhan, China).

2.2. Synthesis and surface modification of UCNPs

$NaYF_4$:Yb, Tm UCNPs were synthesized by the previous method.[33] A mixture of 264 mg YAc_3, 76 mg $YbAc_3$ and 8.36 mg $TmAc_3$ was dissolved in a 100 mL flask containing 17 mL 1-octadecene and 6 mL oleic acid (OA), and the solution was mixed evenly under stirring. The mixture was heated to 100 °C within 10 min in a degassed state, and then it was heated to 160 °C and placed under argon for 30 min followed by natural cooling to room temperature. Then, 10 mL of methanol solution with ammonium fluoride (148 mg) and sodium hydroxide (100 mg) was added slowly to the above solution followed by stirring for 30 min. To remove excess methanol reagent, the solution was heated to 80 °C for 50 min. Subsequently, the solution was continuously heated to 100 °C for 10 min under vacuum. Finally, the reaction system was directly heated to 300 °C and kept for 1 h in argon and then slowly cooled to room temperature. Thirty milliliters of ethanol was added to the mixture by ultrasonic treatment for several minutes, and the white precipitate was collected *via* centrifugation for 10 min (10 621 rcf, 25 °C). The above operation was repeated four times, and the final oil-soluble OA capped UCNPs (OA-UCNPs) obtained were dried in the drying oven at 37 °C and stored in a dryer for future use.

The ligand exchange method was used to modify the surface of the oil-soluble OA-UCNPs *via* the introduction of carboxylic acid groups for increasing the hydrophilicity of the material. The oil-soluble OA-UCNPs were modified into the water-soluble polyacrylic acid (PAA) capped UCNPs (PAA-UCNPs). First, 0.5 g of PAA and 10 mL of diethylene glycol were taken in a 100 mL flask followed by heating to 110 °C under stirring for 1 h in argon. Subsequently, 30 mg of OA-UCNPs were dispersed in 2 mL of toluene solution by ultrasonic treatment for 5 min and were quickly added into the above mixture in a flask kept at 110 °C for another 1 h by stirring vigorously to evaporate the toluene. Finally, the solution was directly heated to 240 °C, stirred for 1 h, and cooled to room temperature. Twenty milliliters of deionized water was added into the mixture by ultrasonic treatment for 5 min, and the precipitate was obtained *via* centrifugation for 10 min (10 621 rcf, 25 °C) to remove the excess PAA and other reagents. The operation was repeated three times and the water-soluble PAA-UCNPs were finally obtained by drying at 37 °C and storing in a dryer for future use.

2.3. Preparation of signal probe and capture probe

The fluorescence signal probe was prepared *via* an active ester method.[33] First, 5 mg of the PAA-UCNPs and 2 mL of 2-(*n*-morpholino)ethanesulfonic acid buffer (MES, 10 mmol L^{-1}, pH 5.5) were mixed in a 10 mL round-bottom flask, and the mixture underwent sonication treatment for 10 min to accelerate the dispersion of PAA-UCNPs. Then, 10 mg of EDC and 5 mg of NHS were added into the above solution and reacted in the bath at 30 °C for 2 h with stirring to activate the carboxylic groups on the surfaces of the PAA-UCNPs. The resultant solution was centrifuged for 10 min (1699 rcf, 4 °C), and the precipitate was washed three times with ultra-pure water. Subsequently, the precipitate was dispersed in 2 mL of *n*-(2-hydroxyethyl)piperazine-*n*-ethanesul-fonic acid buffer (HEPES, 10 mmol L^{-1}, pH 7.2) with 40 μg of BPA antibody. The mixture was incubated for 12 h at 4 °C followed by the addition of BSA (15 mg) and continued the incubation for 1 h at room temperature to prevent the occurrence of non-specific reactions. Then, the white precipitate was collected by centrifugation followed by washing three times using the HEPES buffer. Finally, 1 mL of HEPES buffer was used to disperse the resultant precipitate and the signal probe was obtained.

The coating antigen (BHPVA-OVA) was prepared according to our previous study.[16] The active ester method was applied in the conjugation of carboxyl-functional magnetic polystyrene microspheres (MPMs) with BHPVA-OVA. Five milligrams of MPMs were added into 1 mL of PBS (0.01 mol L^{-1}, pH 7.4) containing 10 mg of EDC and 5 mg of NHS, and the mixture was shaken (240 rpm) for 2 h on a shaking table. After magnetic separation by washing three times with PBS, the precipitate was dispersed in 1 mL of PBS followed by the addition of BHPVA-

OVA (50 μg). The resultant mixture was stirred slowly at room temperature for 4 h. The coating antigen with magnetic polystyrene microsphere conjugate (BHPVA-OVA-MPM) was then treated by adding 15 mg of BSA to prevent the occurrence of non-specific reactions. Afterward, the conjugated complex was collected by magnetic separation followed by washing five times using PBS. Finally, 5 mL of PBS was used to disperse the resultant complex, and the capture probe was obtained.

2.4. Immunoassay procedure

The test principle of the fluorescence immunoassay is shown in Fig. 1. The capture probe and signal probe were added to the sample solution. When BPA was not present in the sample, all the capture probes coupled with the signal probes and the complexes of the capture probes and signal probes obtained by magnetic separation caused the strongest fluorescence signal with excitation at 980 nm. When BPA was present in the sample, the BPA competed with BHPVA-OVA on the surface of the capture probe to couple the anti-BPA antibody on the surface of the signal probe. The amount of complexes of the capture probes and signal probes obtained by magnetic separation decreased with the increasing content of BPA in the sample. This resulted in the fluorescent signal to gradually decrease. There was a correlation between the BPA concentration and the fluorescence signal, and it can be applied to obtain the concentration of BPA in the sample.

The assay test was achieved as follows. First, 100 μL of the BPA standard solution or sample solution and 100 μL of the capture probe were added to a 2 mL centrifuge tube, and 100 μL of the signal probe was subsequently added. The mixture was incubated for 50 min at room temperature on the shaking table. The precipitate was separated by an external magnet and underwent washing three times with PBS. The resulting precipitate was redispersed in 400 μL of PBS, and the fluorescence intensity at 454 nm was measured using a fluorescence spectrometer equipped with an external 980 nm excitation source with a scan speed of 1500 nm min^{-1}.

2.5. Sample preparation

The barreled drinking water samples were collected from the civilian water-supply station. The bottled mineral water samples were purchased from local supermarkets. The river water samples were collected from the local river. For the proposed method, the water samples needed no further treatment to be analyzed. For the recovery study, the samples were spiked with BPA at 0.1, 1, 10, and 100 μg L^{-1} and analyzed simultaneously by the proposed method and HPLC to estimate the accuracy of the proposed method. For HPLC analysis,

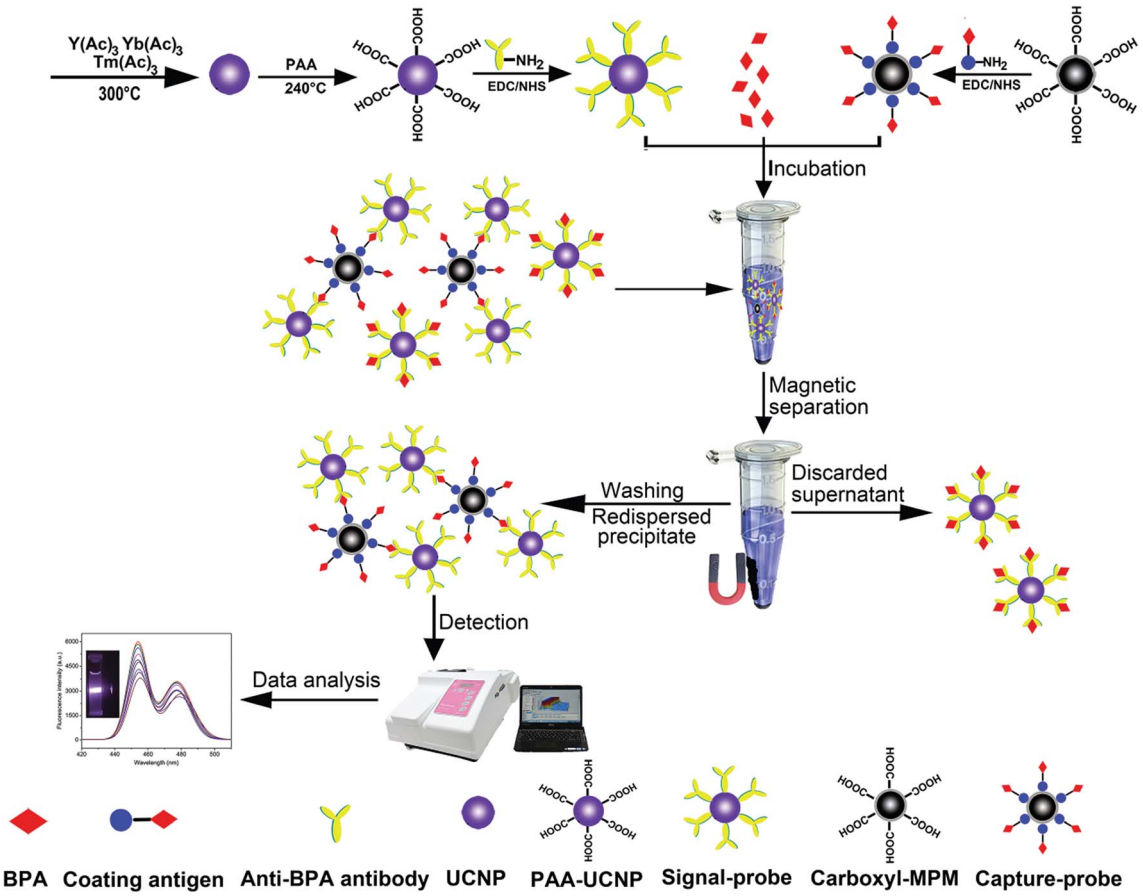

Fig. 1 Schematic illustration of the fluorescence immunoassay.

10 mL of water samples and 10 mL of dichloromethane were mixed and vortexed vigorously for 5 min. The organic phase below the aqueous phase was collected and dried with a stream of nitrogen at 37 °C. The residue was redissolved in 250 μL of methanol and the mixture was vortexed on a vortexer for 5 min and passed through a 0.22 μm filter to be analyzed by HPLC, which was carried out according to our previous study.[16]

3. Results and discussion

3.1. UCNPs characterization

As shown in Fig. 2a and b, the TEM images show that the synthesized UCNPs are spherical, and they have uniform diameters (about 35 nm and 40 nm) and a smooth surface. It should be noted that the synthesis of the spherical UCNPs materials required stringent control of the reaction temperature and time. The fluorescence emission spectra of the synthesized UCNPs are shown in Fig. 2c. These UCNPs showed strong fluorescence intensity and a maximum emission peak at 454 nm with excitation at 980 nm. The results of FTIR analysis in Fig. 2d indicated that a broad band appeared at around 3434 cm^{-1}, which corresponded to the stretching vibration of the hydroxyl group (–OH). A strong band at approximately 2872 cm^{-1} was assigned to the stretching vibration of the methyl group ($–CH_3$) that existed on the surface of the OA-UCNPs. After ligand exchange with PAA, this feature was replaced and a new characteristic peak at 1734 cm^{-1} appeared in the spectrum of the PAA-UCNPs, reflecting the successful introduction of the carboxyl groups (–COOH) on the PAA-UCNPs surface. Fig. 2e shows the XRD pattern of the OA-UCNPs and PAA-UCNPs. Compared to the standard XRD pattern of the β-phase $NaYF_4$ (JCPDS card 16-0334), the structures of the OA-UCNPs and PAA-UCNPs were basically consistent with the results of the standard.

3.2. Optimization of working parameters

To achieve the best test performance, the conjugation amounts of the coating antigen with MPMs and of the anti-BPA antibody with PAA-UCNPs were optimized. Various amounts of coating antigen (30, 40, 50, 60, 70, and 80 μg) were respectively added into 1 mL of the activated MPMs solution to prepare the capture probe. By magnetic separation, the supernatant was collected to detect the amount of unconjugated coating antigen using the BCA protein quantitation kit. The amount of conjugated coating antigen was calculated as the difference between the total added amount of coating antigen and the amount of unconjugated coating antigen. The conjugation rate $\left(\text{conjugation rate } (\%) = \frac{m_c}{m_t} \times 100\%\right)$ is expressed as a percentage (%, w/w), wherein m_t is the total added amount of coating antigen and m_c is the amount of conjugated coating antigen. As shown in Fig. 3a, the amount of conjugated coating antigen increased with the increase in the added amount of coating antigen. The amount of conjugated coating antigen reached saturation with the increase in the added amount when the added amount of coating antigen was equal to or more than 50 μg. The conjugation rate (%) decreased with the increase in the added amount of coating antigen. The best conjugate efficiency with an 86% conjugation rate was achieved when the added amount of coating antigen was 50 μg. Finally, 50 μg of the

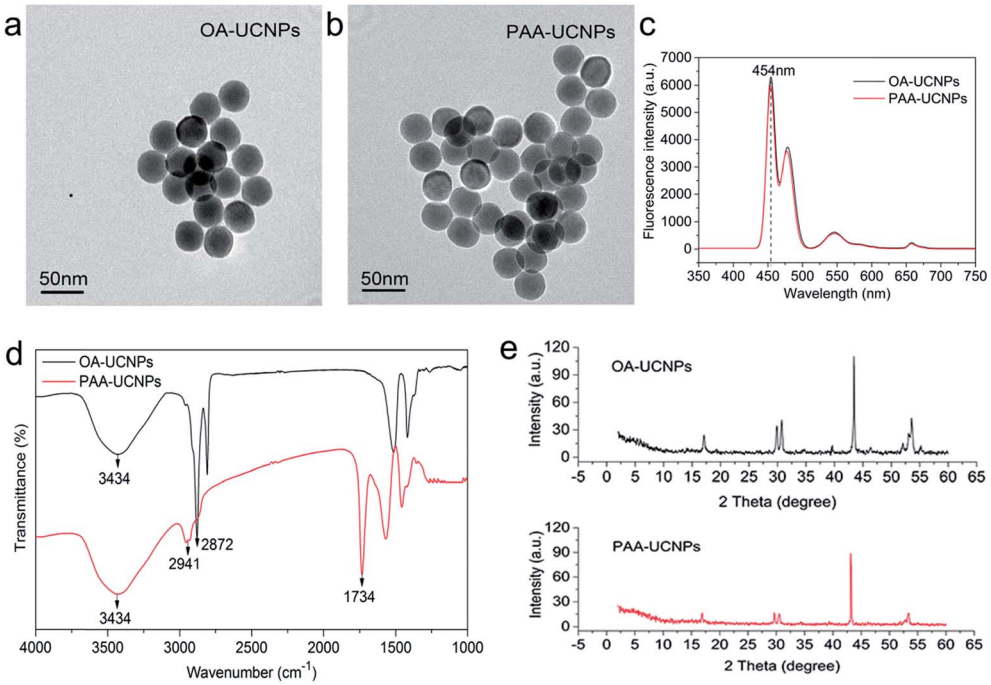

Fig. 2 Characterization of the synthesized UCNPs. Transmission electron microscope (TEM) images (a and b), fluorescence emission spectra (c), fourier-transform infrared (FT-IR) spectra (d) and X-ray diffraction (XRD) patterns (e).

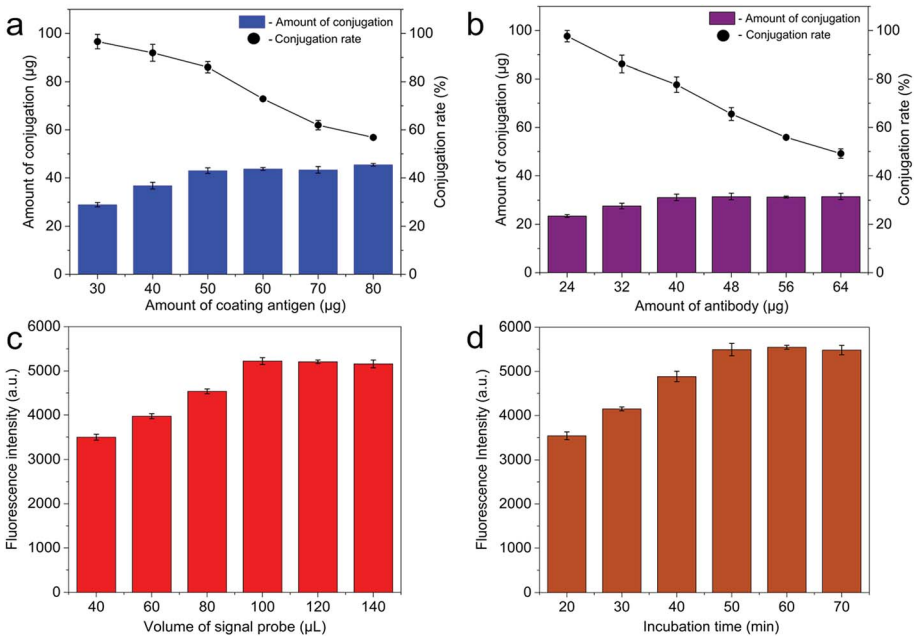

Fig. 3 Optimization of the working parameters. (a) Optimization of the amount of coating antigen conjugated with MPMs in capture probes. (b) Optimization of the amount of antibody conjugated with PAA-UCNPs in signal probes. (c) Optimization of the added volume of the signal probe in the test process with 100 μL of the capture probe. (d) Optimization of the incubation time of the signal probe, capture probe and sample solution. Each data point is the mean of three replicates.

added amount of coating antigen was used to prepare the capture probe.

Similarly, to optimize the amount of antibody, varying amounts of anti-BPA antibody (24, 32, 40, 48, 56, and 64 μg) were respectively added into 2 mL of the activated PAA-UCNPs solution to prepare the signal probe. The supernatant was collected by centrifugation to detect the amount of unconjugated antibody using the BCA protein quantitation kit. The amount of conjugated antibody was calculated as the difference between the total added amount of antibody and the amount of unconjugated antibody. The conjugation rate $\left(\text{conjugation rate } (\%) = \frac{m_c}{m_t} \times 100\%\right)$ is expressed as a percentage (%, w/w), wherein m_t is the total added amount of antibody and m_c is the amount of conjugated antibody. As shown in Fig. 3b, the amount of conjugated antibody increased with the increase in the added amount of antibody. The amount of conjugated antibody reached saturation with the increase in the added amount when the added amount of antibody was equal to or more than 40 μg. The conjugation rate (%) decreased with increasing added amount of antibody. The best conjugate efficiency, with a 77.7% of conjugation rate, was achieved when the added amount of antibody was 40 μg. Finally, 40 μg of the added amount of antibody was used to prepare the signal probe.

Subsequently, the added volume of the signal probe and the incubation time were optimized to achieve the best assay performance. Varying added volumes of the signal probe (40, 60, 80, 100, 120, and 140 μL) were applied during a test with an incubation time of 60 min. The fluorescence intensity increased with the increase in the added volume of the signal probe, and the fluorescence intensity was the strongest when the added volume of the signal probe was equal to or more than 100 μL (Fig. 3c). Finally, 100 μL of the signal probe was applied in this assay to achieve optimal assay performance. The assay was performed at varying incubation times (20, 30, 40, 50, 60, and 70 min). The fluorescence intensity increased with the increase in the incubation time, and the fluorescence intensity was the strongest when the incubation time was equal to or more than 50 min (Fig. 3d). Finally, an incubation time of 50 min was applied in this assay to achieve the best assay performance.

3.3. Development of fluorescence immunoassay

Under optimal conditions, a series of BPA standard solutions (0, 0.1, 0.5, 1, 5, 10, 50, 100, and 500 μg L^{-1}) was detected by the proposed assay to evaluate the sensitivity of the assay. There was a correlation between the concentrations of BPA and the decreased fluorescence intensities (ΔI). The ΔI value was calculated by the formula: $\Delta I = I_0 - I$, wherein I_0 is the upconversion fluorescence intensity in the absence of BPA and I is the upconversion fluorescence intensity in the presence of BPA. When BPA was absent in the test system, the fluorescence intensity was maximized. The fluorescence intensity decreased with the increase in the BPA concentration. Fig. 4 shows the standard curve of the proposed assay. The linear range was from 0.1 to 500 μg L^{-1} with a linear equation of $y = 204.73 \ln(x) + 647.09$ ($R^2 = 0.9954$). The LOD value was calculated by the formula: LOD $= 3\sigma/s$, wherein σ is the standard deviation of blank signals ($n = 6$) and s is the slope of the standard curve.[34]

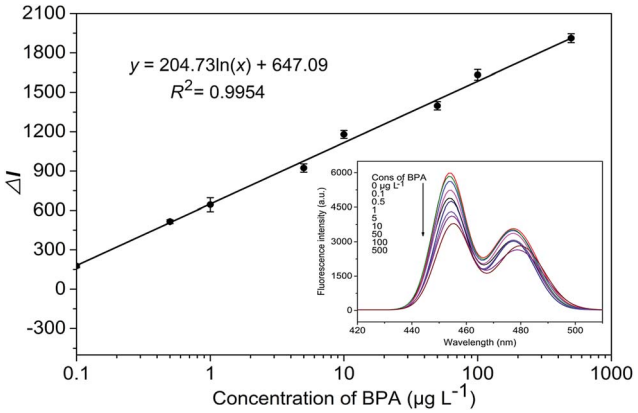

Fig. 4 Standard curve of the fluorescence immunoassay for BPA in the assay buffer. Inset: fluorescence intensity of the immune complexes in the absence of BPA and in the presence of varying concentrations of BPA. Each data point is the mean of three replicates.

The LOD of the proposed method for the detection of BPA in the assay buffer was 0.02 μg L^{-1}.

3.4. Specificity of assay

To estimate the specificity of the proposed assay, the values of the change in fluorescence intensity in the absence and in the presence of BPA or other analogues (500 μg L^{-1}) were simultaneously detected by the proposed assay. As shown in Fig. 5, compared with BPA, several analogues including bisphenol E, bisphenol C, bisphenol S, bisphenol G, phenolphthalein, and tetrabromobisphenol A caused very low fluorescence intensity changes, indicating that the proposed assay cannot recognize those analogues and that they have no effect on the assay. Both 4,4-dihydroxydiphenylmethane and 4,4-dihydroxybenzophenone caused relatively low changes in fluorescence intensity, but these low changes were negligible and would not affect the specific trace analysis of BPA.

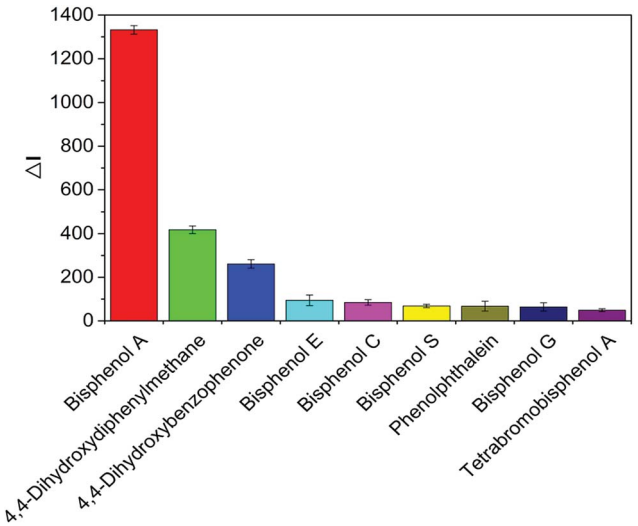

Fig. 5 Specificity analysis of the fluorescence immunoassay. Each data point is the mean of three replicates.

3.5. Sample analysis

The barreled water, bottled mineral water, and river water samples were certified as negative BPA samples by HPLC and were spiked with BPA at four levels (0.1, 1, 10, and 100 μg L^{-1}). To evaluate the assay accuracy, the proposed fluorescence immunoassay and HPLC were simultaneously applied to analyze the spiked water samples. As shown in Table 1, the recoveries of BPA ranged from 85.35% to 108.35% for the proposed fluorescence immunoassay and from 81.60% to 113.72% for HPLC. The proposed fluorescence immunoassay showed good accuracy for the detection of BPA with good correlation (R^2 = 0.9906) between the results obtained by our assay and HPLC. The indirect competitive enzyme-linked immunosorbent assay (ELISA) using the anti-BPA polyclonal antibody and coating antigen (BHPVA-OVA) has been developed. The half-maximum inhibition concentration (IC_{50}) value of BPA and the limit of detection (LOD, concentration calculated as IC_{15}) of this ELISA are 45 μg L^{-1} and 1.9 μg L^{-1}, respectively, for BPA in phosphate-buffered saline (PBS). The standard curve of this ELISA is shown in ESI Fig. S2.† A 2-fold dilution with PBS for the water sample will allow minimal interference of the matrix on the ELISA. The LOD of this ELISA for the water sample is 3.8 μg L^{-1}. In this study, the proposed method was rapid, convenient, and sensitive, allowing for the water samples to be analyzed directly *via* developed fluorescence immunoassay without any pretreatment. The LOD of BPA for the proposed method in the water samples is 0.02 μg L^{-1}, which is far lower than the LOD of the ELISA (3.8 μg L^{-1}). When the same anti-BPA polyclonal antibody and coating antigen (BHPVA-OVA) are used to develop the ELISA and fluorescence immunoassay, the developed fluorescence immunoassay shows higher sensitivity.

3.6. Analysis and validation of bisphenol A in real water samples

Ten barreled water samples, 10 bottled mineral water samples, and 10 river water samples were collected, and the concentrations of BPA were analyzed by the proposed method to investigate the practicability of this method. Meanwhile, HPLC was applied to analyze the concentrations of BPA in these water samples to validate the reliability of the proposed fluorescence immunoassay. BPA was not found in the collected bottled mineral water samples. Low concentrations of BPA were detected in two barreled water samples and one river water sample (Table 2). The concentrations of BPA detected by this method in the barreled water no. 1, barreled water no. 2, and river water samples were 153.33, 144.09, and 182.43 ng L^{-1}, respectively. Simultaneously, HPLC had validated the presence of BPA in these water samples with concentrations of 161.20, 139.71, and 176.86 ng L^{-1}, respectively. These consistent results proved the reliability of the proposed fluorescence immunoassay to detect BPA in real water samples.

The presence of BPA in the river water sample can be ascribed to environmental pollution, while the presence of BPA in the barreled drinking water samples may have been caused by background BPA in water sources or the release and

Table 1 Recoveries of bisphenol A from spiked samples by the proposed method and HPLC ($n = 3$)

Sample	Spiked level ($\mu g\ L^{-1}$)	This method		HPLC	
		Recovery (%)	CV (%)[a]	Recovery (%)	CV (%)
Barreled water	0.1	106.89	12.94	89.06	1.56
	1	85.35	17.37	97.70	3.36
	10	105.09	11.57	110.82	7.60
	100	85.99	0.40	104.88	0.49
Bottled mineral water	0.1	102.60	14.33	85.18	3.68
	1	96.44	5.77	92.78	0.88
	10	104.75	15.52	107.64	12.60
	100	108.35	7.22	100.18	1.19
River water	0.1	102.63	2.21	81.60	3.44
	1	86.75	9.27	92.68	4.55
	10	100.41	16.04	113.72	2.33
	100	103.86	8.39	91.73	1.59

[a] Coefficient of variation.

Table 2 Analysis of bisphenol A in real water samples by the proposed method and HPLC ($n = 3$)

Sample	Measured ($ng\ L^{-1}$) (mean ± SD[a])	
	This method	HPLC
Barreled water no. 1	153.33 ± 16.78	161.20 ± 18.59
Barreled water no. 2	144.09 ± 12.45	139.71 ± 7.13
River water	182.43 ± 21.27	176.86 ± 8.99

[a] Standard deviation.

transference of BPA from plastic packing materials. The illegal recycling of discarded plastic packing materials may result in the transference of BPA to the water. Although the concentrations of BPA detected in these water samples were all lower than 0.01 mg L^{-1} (the concentration limit established in the Standards for Drinking Water Quality (GB 5749-2006) of China), considering the toxicity of BPA, long-term drinking may lead to health risks for humans.

4. Conclusions

In our study, water-soluble carboxyl-functional $NaYF_4$:Yb/Tm UCNPs with emissions at 454 nm excited by a 980 nm laser were used as the fluorescence signal labels. The magnetic polystyrene microspheres (MPMs) were chosen as separation mediums to separate the immunocomplex from the test system. The magnetic separation operation *via* an external magnet was simpler and more time-saving than centrifugation. Water samples without any pretreatment can be analyzed directly, and the LOD of BPA in the water samples was 0.02 $\mu g\ L^{-1}$. The results of the spiked and real water samples by the proposed fluorescence immunoassay were in good agreement with the results obtained by HPLC, indicating good accuracy and practicability of the proposed method. With a simple and rapid analysis process, the proposed upconversion nanoparticles-based fluorescence immunoassay in combination with magnetic separation can be applied to rapidly and accurately detect trace levels of BPA in drinking and environmental water. Low concentrations of BPA have been detected in the real barreled, drinking and river water samples in this study. Although the concentration of BPA in the drinking water was very low, long-term drinking may lead to health risks for humans. Therefore, it is necessary to strictly control the discharge of the wastewater containing BPA into the environment and the landfills of discarded plastic packing material garbage to avoid contaminating the drinking water source. In addition, it is also necessary to strictly control the illegal recycling of discarded plastic packing materials in order to prevent the release and transfer of BPA from packing materials to drinking water or food. The proposed fluorescence immunoassay can serve as a useful detection tool for the simple, rapid, sensitive, and accurate monitoring of BPA contamination in the drinking and environmental water sources.

Conflicts of interest

There are no conflicts to declare.

Acknowledgements

This study was supported by the Tianjin Municipal Science and Technology Commission (Project No. 16PTSYJC00130), the National Key R&D Program of China (Project No. 2016YFD0401204), the National Natural Science Foundation of China (Project No. 31501566), and the International Science and Technology Cooperation Program of China (Project No. 2014DFR30350).

References

1 A. Izzotti, S. Kanitz, F. D'Agostini, A. Camoirano and F. S. De, *Mutat. Res., Genet. Toxicol. Environ. Mutagen.*, 2009, **679**, 28–32.

2 T. Yamamoto, A. Yasuhara, H. Shiraishi and O. Nakasugi, *Chemosphere*, 2001, **42**, 415–418.
3 F. S. vom Saal and W. V. Welshons, *Environ. Res.*, 2006, **100**, 50–76.
4 C. A. Staples, P. B. Dorn, G. M. Klecka, S. T. O'Block and L. R. Harris, *Chemosphere*, 1998, **36**, 2149–2173.
5 J. H. Kang, F. Kondo and Y. Katayama, *Toxicology*, 2006, **226**, 79–89.
6 R. Mercogliano and S. Santonicola, *Food Chem. Toxicol.*, 2018, **114**, 98–107.
7 A. García-Prieto, M. L. Lunar, S. Rubio and D. Pérez-Bendito, *Anal. Chim. Acta*, 2008, **630**, 19–27.
8 S. C. Cunha, C. Oliveira and J. O. Fernandes, *Anal. Bioanal. Chem.*, 2017, **409**, 151–160.
9 X. L. Cao and S. Popovic, *Food Addit. Contam., Part A*, 2018, **35**, 49–55.
10 J. Q. Xue, D. W. Li, L. L. Qu and Y. T. Long, *Anal. Chim. Acta*, 2013, **777**, 57–62.
11 S. X. Zhong, S. N. Tan, L. Y. Ge, W. P. Wang and J. R. Chen, *Talanta*, 2011, **85**, 488–492.
12 J. D. Huang, X. M. Zhang, S. Liu, Q. Lin, X. R. He, X. R. Xing and W. J. Lian, *J. Appl. Electrochem.*, 2011, **41**, 1323–1328.
13 W. B. Miao, B. W. Wei, R. J. Yang, C. H. Wu, D. Lou, W. Jiang and Z. J. Zhou, *New J. Chem.*, 2014, **38**, 669–675.
14 J. J. Manclús, M. J. Moreno and Á. Montoya, *Anal. Methods*, 2013, **5**, 4244–4251.
15 Z. L. Mei, Y. Deng, H. Q. Chu, F. Xue, Y. H. Zhong, J. J. Wu, H. Yang, Z. C. Wang, L. Zheng and W. Chen, *Microchim. Acta*, 2013, **180**, 279–285.
16 W. Sheng, Y. Liu, S. J. Li, Y. Lu, Q. Chang, Y. Zhang and S. Wang, *Food Analytical Methods*, 2018, **11**, 675–685.
17 Y. Lu, M. J. Li, M. L. Ding, G. Z. Liu, Y. Zhang and S. Wang, *J. Electroanal. Chem.*, 2016, **779**, 34–38.
18 K. Hegnerová, M. Piliarik, M. Šteinbachová, Z. Flegelová, H. Černohorská and J. Homola, *Anal. Bioanal. Chem.*, 2010, **398**, 1963–1966.
19 Z. Lei, Y. S. Chen, Z. W. Liu, W. J. Ji and S. Q. Zhao, *Pigm. Resin Technol.*, 2018, **47**, 38–46.
20 C. J. Hou, L. X. Zhao, F. L. Geng, D. Wang and L. H. Guo, *Anal. Bioanal. Chem.*, 2016, **408**, 8795–8804.
21 X. L. Wu, L. B. Wang, W. Ma, Y. Y. Zhu, L. G. Xu, H. Kuang and C. L. Xu, *Immunol. Invest.*, 2012, **41**, 38–50.
22 P. N. Huang, S. Q. Zhao, S. A. Eremin, S. W. Zheng, D. Lai, Y. S. Chen and B. Guo, *Anal. Methods*, 2015, **7**, 4246–4251.
23 T. Z. Guan, T. Z. Li, T. H. Zhang, Z. L. Li, Y. Z. Wang, H. S. Yu, P. Ruan, J. Zhang and Y. J. Wang, *Int. J. Food Prop.*, 2017, **20**, 1920–1929.
24 J. Zhang, S. Q. Zhao, K. Zhang and J. Q. Zhou, *Chemosphere*, 2014, **95**, 105–110.
25 D. Genovese, E. Rampazzo, S. Bonacchi, M. Montalti, N. Zaccheroni and L. Prodi, *Nanoscale*, 2014, **6**, 3022–3036.
26 G. S. Yi and G. M. Chow, *Adv. Funct. Mater.*, 2006, **16**, 2324–2329.
27 T. Guo, Q. L. Deng, G. Z. Fang, C. C. Liu, X. Huang and S. Wang, *Biosens. Bioelectron.*, 2015, **74**, 498–503.
28 P. Zhang, S. Rogelj, K. Nguyen and D. Wheeler, *J. Am. Chem. Soc.*, 2006, **128**, 12410–12411.
29 N. Duan, S. J. Wu, C. Q. Zhu, X. Y. Ma, Z. P. Wang, Y. Yu and Y. Jiang, *Anal. Chim. Acta*, 2012, **723**, 1–6.
30 S. J. Wu, N. Duan, C. Q. Zhu, X. Y. Ma, M. Wang and Z. P. Wang, *Biosens. Bioelectron.*, 2011, **30**, 35–42.
31 S. Shikha, X. Zheng and Y. Zhang, *Nano–Micro Lett.*, 2018, **10**, 31.
32 G. S. Hu, W. Sheng, Y. Zhang, X. N. Wu and S. Wang, *Anal. Bioanal. Chem.*, 2015, **407**, 8487–8496.
33 C. H. Liu, Z. Wang, X. K. Wang and Z. P. Li, *Sci. China: Chem.*, 2011, **54**, 1292–1297.
34 X. L. Wu, Y. Song, X. Yan, C. Z. Zhu, Y. Q. Ma, D. Du and Y. H. Lin, *Biosens. Bioelectron.*, 2017, **94**, 292–297.

